

# *Characterisation of $\beta$ -lactoglobulin nanoparticles and their binding to caffeine*

Article

Accepted Version

Creative Commons: Attribution-Noncommercial-No Derivative Works 4.0

Guo, Y., Harris, P., Kaur, A., Pastrana, L. and Jauregi, P. (2017) Characterisation of  $\beta$ -lactoglobulin nanoparticles and their binding to caffeine. *Food Hydrocolloids*, 71. pp. 85-93. ISSN 0268-005X doi: <https://doi.org/10.1016/j.foodhyd.2017.04.027> Available at <https://centaur.reading.ac.uk/71055/>

It is advisable to refer to the publisher's version if you intend to cite from the work. See [Guidance on citing](#).

Published version at: <http://dx.doi.org/10.1016/j.foodhyd.2017.04.027>

To link to this article DOI: <http://dx.doi.org/10.1016/j.foodhyd.2017.04.027>

Publisher: Elsevier

All outputs in CentAUR are protected by Intellectual Property Rights law, including copyright law. Copyright and IPR is retained by the creators or other copyright holders. Terms and conditions for use of this material are defined in the [End User Agreement](#).

[www.reading.ac.uk/centaur](http://www.reading.ac.uk/centaur)

**CentAUR**

Central Archive at the University of Reading

Reading's research outputs online



## Characterisation of $\beta$ -Lactoglobulin nanoparticles and their binding to caffeine

<sup>1</sup>Yuchen Guo <sup>2</sup>Peter Harris, <sup>3</sup>Lorenzo Pastrana, <sup>1\*</sup>Paula Jauregi

<sup>1</sup>Department of Food and Nutritional Sciences. University of Reading, Whiteknights, Reading, RG6 6AP, United Kingdom.

<sup>2</sup>Centre for Advanced Microscopy, University of Reading, Whiteknights, Reading, RG6 6AP, United Kingdom

<sup>3</sup>INL - International Iberian Nanotechnology Laboratory, Av. Mestre José Veiga s/n, 4715-330 Braga Portugal

\*Corresponding author.

E-mail address: [p.jauregi@reading.ac.uk](mailto:p.jauregi@reading.ac.uk) (P.Jauregi)

Address: Department of Food and Nutritional Sciences. University of Reading, Whiteknights, Reading, RG6 6AP, United Kingdom.

Telephone: +44(0)1183788728

### 1 **ABSTRACT**

2 The production of  $\beta$ -Lg nanoparticles by a simple heat-induced denaturation method  
3 without the need to add chemicals was performed at different conditions of pH, and  
4 temperature of denaturation. Optimum conditions were set as 0.2 %  $\beta$ -Lg, pH 6 and  
5 simply heating at 75°C for 45 minutes. At these conditions, a monodisperse solution  
6 with colloidal stability was obtained and the yield of aggregation was over 90%. Shape  
7 and size of nanoparticles were determined by Dynamic Light Scattering and by electron  
8 microscopy. A monodisperse particle size distribution of spherical shape particles  
9 (200nm-300nm diameter) was obtained. The stability of the aggregates towards  
10 various types of dissociating buffers was studied. Sodium dodecyl sulphate (SDS) and  
11 urea had a strong effect on the size of the nanoparticles, while 2-Mercaptoethanol and  
12 Dithiothreitol (DTT) had no significant effect. Therefore hydrogen bonding and  
13 hydrophobic interactions were the predominant interactions responsible for the

14 microstructure. Maximum yield of caffeine encapsulation of 13.54% was obtained at  
15 caffeine to the  $\beta$ -Lg molar ratio of 50:1. Rapid nanoparticle degradation and increase  
16 in polydispersity during the incubation of  $\beta$ -Lg nanoparticles at simulating stomach  
17 conditions was observed due to enzymatic attack. Nevertheless, little release of  
18 entrapped caffeine was noted. Total release was achieved at intestinal conditions.  
19 Finally, the adsorption of caffeine to both native and denatured  $\beta$ -Lg followed a  
20 Langmuir adsorption isotherm model and caffeine had three times more affinity for  
21 partially denatured  $\beta$ -Lg in nanoparticles than for native protein.

22

23 **Keywords:** Caffeine; nanoparticles;  $\beta$ -Lactoglobulin; simulated digestion,  
24 encapsulation.

## 25 **1. Introduction**

26 Whey is the principal by-product of cheese manufacturing and it represents 85-95% of  
27 the initial volume of processed milk with high Chemical oxygen demand (COD) and  
28 Biochemical oxygen demand (BOD) values hence its disposal would have a negative  
29 environmental impact. The total world production of liquid cheese whey in 2008 was  
30 in the region of 187 million metric tons and of this 3.2 million metric tons were  
31 industrially utilised and processed into higher added value products such as, whey  
32 powder, whey proteins concentrates and whey protein fractions (Afferstsholt & Palmer,  
33 2009; C. Baldasso , T.C. Barros, & Tessaro, 2011); the remaining whey is used for  
34 animal feed, fertilisers, baby milk powder and some it is just dumped. Whey is a  
35 valuable source of proteins (about 0.8-0.9% protein) with high nutritional value and  
36 additional biological properties as well as numerous functional properties such as  
37 gelation, emulsifying and foaming properties(Jauregi & Welderufael, 2010). The major  
38 whey protein, beta-lactoglobulin ( $\beta$ -Lg) which comprises 51 % (w/w) of total protein  
39 has very interesting aggregation properties which have been exploited for its application  
40 as an encapsulant (Chen, Remondetto, & Subirade, 2006; H. J. Giroux, Houde, &  
41 Britten, 2010; Jones, Lesmes, Dubin, & McClements, 2010). This protein is  
42 predominantly dimeric at physiological conditions, but dissociates to a monomer at

43 about pH 3 (Tauliera & Chalikian, 2001); its isoelectric point (pI) is 5.13. Four out of  
44 its five cysteine residues form two disulfide bridges leaving a free reactive thiol group  
45 that appears to be responsible for the formation of covalent aggregates upon heating  
46 (Sawyer, 2002). Also  $\beta$ -Lg possess a hydrophobic pocket that when exposed by, for  
47 example, heat denaturation forms aggregates by hydrophobic interactions. These  
48 aggregation properties can be manipulated by changing temperature, pH, and ionic  
49 strength. Under prolonged heating at low pH and low ionic strength, a transparent 'fine-  
50 stranded' gel is formed, in which the protein molecules assemble into long stiff fibers  
51 and also can produce nanoparticles (Ko & Gunasekaran, 2006).

52 Food protein-based nanoparticles are of great interest because they are Generally  
53 Recognised as Safe (GRAS), easy to prepare, no need for chemical cross-linking agents  
54 during preparation, better control over size distributions (Chen et al., 2006;  
55 Gunasekaran, Ko, & Xiao, 2006).  $\beta$ -Lg is able to aggregate forming nanoparticles that  
56 have some technological advantages as an encapsulant for bioactives; among others:  
57 inexpensive, food grade and non-toxic material, capable of solubilizing and protecting  
58 hydrophobic biologically active molecules in aqueous media as well as capable of  
59 retaining sensory qualities, and promote bioavailability of hydrophobic biologically  
60 active molecules. In this sense, when electrically charged,  $\beta$ -Lg is also able to ion  
61 binding and electrostatic complex formation, self and co-assembly and covalent  
62 conjugation (Livney, 2010).

63 In previous works,  $\beta$ -Lg nanoparticles have been applied as carriers for a range of  
64 nutraceutical products such as, polysaccharides, pectin, carageenan or chitosan (Chen  
65 & Subirade, 2005; Jones et al., 2010; Ron, Zimet, Bargarum, & Livney, 2010; Zimet &  
66 Livney, 2009) where  $\beta$ -Lg forms complexes with each of these products. The  
67 complexity of method and materials used for the production of such complexes hinders  
68 the possibility for scaling up production. On the other hand, simple production steps  
69 such as desolvation with ethanol can produce nanoparticles without application of heat,  
70 thus making it very feasible for heat-labile bioactive components (Gulseren, Fang, &

71 Corredig, 2012). Nonetheless, usage of organic solvents for food application is still the  
72 major drawback for this method (Nicolai, Britten, & Schmitt, 2011).

73 Caffeine is an amphiphilic alkaloid drug that has a strong bioactivity acting as a  
74 stimulant drug of the central nervous system. For this reason is considered the most  
75 popular legal stimulant consumed in the world, mainly in the form of coffee and tea  
76 infusion (Gilbert, 1984). In the last years, several energy drinks containing caffeine  
77 have been launched to the market having a great success and customer acceptance  
78 (Somogyi, 2010). Unfortunately, caffeine has very bitter taste and unpleasant aftertaste  
79 limiting or even excluding their use from many food and drink formulations.  
80 Encapsulation of caffeine enables bitterness masking and it can be easily added to food  
81 and drink products without changing the flavour or increasing the bitterness level. In  
82 addition, encapsulation could provide protection against harsh processing conditions  
83 and controlled release.

84 The aim of this study is to investigate the production of  $\beta$ -Lg nanoparticles by a simple  
85 heat-induced denaturation method without the need to add chemicals and/or other  
86 reagents and to investigate their application to the encapsulation of caffeine. Particles  
87 were characterised in terms of size by Dynamic Light Scattering technique,  
88 fluorescence and by electron microscopy. Stability to buffers was examined as an  
89 indirect measurement of the internal forces responsible for the molecular network  
90 within the particles. This led to an improved understanding of the mechanism of  
91 aggregate formation and their interactions with caffeine.

92

## 93 **2. Materials and Methods**

94

### 95 **2.1. Materials**

96  $\beta$ -lactoglobulin ( $\beta$ -Lg) from bovine milk,  $\geq 90\%$  PAGE lyophilised powder was  
97 purchased from Sigma-Aldrich (United Kingdom) for all the experiments. The material  
98 used for encapsulation was caffeine (99% purity) obtained also from Sigma-Aldrich  
99 (United Kingdom).

100

101

## 102 **2.2. Methods**

103

### 104 **2.2.1. Preparation of $\beta$ -lactoglobulin nanoparticle**

105 The  $\beta$ -lg powder was dispersed in deionized water to make 50 ml 0.2 % w/v  $\beta$ -Lg stock  
106 solution and it was stirred magnetically for about two hours at room temperature. This  
107 stock solution was stored in a 50ml Falcon tube (VWR International, 525-0403, USA)  
108 at 4°C over the whole night to complete hydration. In order to prevent the growth of  
109 microorganisms, 200 ppm sodium azide were added.

110 A 5 ml sample from the  $\beta$ -Lg stock solution was added into 15ml a Falcon tube (VWR  
111 International, 5250401, USA) and after warming the sample up to room temperature,  
112 the pH was measured. Then the pH of the sample was adjusted to 6.0 (except when the  
113 pH effect was investigated) using a pH meter (Mettler Toledo, Switzerland) with 0.1M  
114 HCL and 0.1M NaOH. After this, the Falcon tube containing the sample was introduced  
115 into a water bath (Grant Instrument Ltd., Cambridge, United Kingdom) that had been  
116 previously heated at 75 °C. The sample was left for 45 minutes at this temperature  
117 except when the effect of heat load was investigated. The temperature of the sample  
118 was monitored and it took about 12-14 minutes for the temperature in the samples to  
119 reach the water temperature (75 °C). After the set heating time samples were moved to  
120 an ice bath for 10 minutes to terminate incubation and the pH of the sample was  
121 measured.

122 For experiments where pH effect (from 5.7 to 6.2) was investigated, nanoparticles were  
123 produced following procedure described above but initial pH of sample was changed.

124 For experiments where temperature effect was investigated, samples were heated at  
125 60 °C and 75°C; all other conditions were kept constant (0.2 % w/w of  $\beta$ -Lg, pH 6 and  
126 heating time 75 minutes). For experiments where the heating time (heat load) effect  
127 was investigated, nanoparticles were produced following procedure described above at  
128 0.2 % w/w of  $\beta$ -Lg, pH 6 and 75°C but at varying heating times: 15, 25, 35, 45, 55, 65  
129 and 75 mins.

130

131

### 132 **2.2.2 Preparation of caffeine encapsulated $\beta$ -lactoglobulin nanoparticles**

133 The experiment on the encapsulation of caffeine was conducted only with 0.2% (w/v)  
134 dispersions. Caffeine (99% purity) was added to the  $\beta$ -Lg dispersions prior to pH  
135 adjustment to obtain 10:1, 20:1, 50:1, 100:1, 200:1 caffeine to  $\beta$ -Lg molar ratios. A  
136 certain volume of stock caffeine solution (10mg/ml) was mixed with protein samples  
137 to achieve 10:1, 20:1 caffeine to  $\beta$ -Lg molar ratios, respectively. The final protein  
138 concentration after pH adjustment and caffeine addition was 0.2 % (w/v). Caffeine  
139 powder was added into samples to obtain 50:1, 100:1, 200:1 caffeine to  $\beta$ -Lg molar  
140 ratios, respectively. Once caffeine was added to the  $\beta$ -Lg solution, the encapsulation  
141 method proceeded in the same way as the nanoparticle formation procedure described  
142 in section 2.2.1.

143

### 144 **2.2.3. Particle size distribution**

145 The z-average hydrodynamic diameter of  $\beta$ -Lg nanoparticles was measured by the  
146 dynamic light scattering technique using Zetasizer Nano Z (Malvern Instruments Inc.,  
147 Malvern, United Kingdom) at  $25 \pm 0.1^\circ\text{C}$  and five measurements were taken for each  
148 sample. The measurement was determined by considering the refractive index of  $\beta$ -Lg  
149 as 1.45 and that of the dispersant medium (deionised water) as 1.33. The z-average  
150 mean was calculated from the intensity of light scattered from the nanoparticles, based  
151 on Stokes-Einstein equation, which assumes that all particles are spherical. Each sample  
152 was measured five times and the mean and standard deviation were determined. In some  
153 cases samples were diluted in order to operate at concentrations appropriate for DLS  
154 (as indicated by the machine). When samples were incubated with different dissociating  
155 buffers the refractive index of these buffers was taken into account: (i) 10M urea,  
156 refractive index 1.370 (Warren & Gordon, 1966) (ii) 0.1M Mercaptoethanol, refractive  
157 index 1.500 (Sigma-Aldrich, 2017), (iii) 1% (w/v) SDS, refractive index 1.334  
158 (Tumolo, Angnes, & Baptista, 2004), (v) 0.1 M DTT, refractive index 1.576 (ChemBK,  
159 2017).



160

161

#### 162 **2.2.4. $\beta$ -lactoglobulin aggregation**

163 The degree of thermal aggregation for  $\beta$ -Lg was determined by separation of denatured  
164  $\beta$ -Lg nanoparticles from native  $\beta$ -Lg using centrifugal ultrafiltration Vivaspin® 20  
165 (Sartorius Stedim Biotech, Germany) with 50kDa molecular weight cut-off membrane.

166 To quantify the amount of native and aggregated  $\beta$ -Lg, 5ml of the heated  $\beta$ -Lg solution  
167 following the method described in section 2.2.1 was centrifuged at 2000 rpm for 15  
168 minutes to collect the retentate as well as the permeate; the retentate and permeate  
169 volumes were determined by weight. The concentration of the native  $\beta$ -Lg remained in  
170 permeate was determined by the bicinchoninic acid (BCA) method. In brief, 0.1 ml of  
171 the permeate solution was added to 2 ml of BCA working reagent (bicinchoninic acid  
172 and copper (II) sulphate pentahydrate), followed by incubation at 37°C for 30 min. The  
173 reaction solution was measured at 562 nm in an Ultrospec ® 1100 pro UV-vis  
174 spectrophotometer (United Kingdom). The percentage of protein aggregated was  
175 determined by measuring the total protein in the permeate followed by mass balance on  
176 protein.

177

#### 178 **2.2.5. Microscopy method**

179 Environmental Scanning Electron Microscopy (ESEM) was carried out on samples  
180 produced at the optimum conditions - 0.2 %  $\beta$ -lactoglobulin, pH 6.0, at 75 °C for 45  
181 minutes. The microscope used was a FEI Quanta 600, operated in environmental mode  
182 with a water vapour pressure of 822.46Pa, and a specimen temperature of 5°C. The  
183 accelerating voltage was 20 kV. One drop of  $\beta$ -lactoglobulin nanoparticles sample was  
184 dispersed at the surface of the metal stub of the microscope and was dry at room  
185 temperature to ensure to some extent that moisture content was evaporated so that  
186 nanoparticles images were easier to capture.

187

#### 188 **2.2.6. Fluorescence measurement of protein solutions**

189 The degree of  $\beta$ -Lg conformational changes on fluorescence emission of tryptophan  
190 (Trp) was accessed by fluorescence spectrophotometer with temperature controller  
191 (Varian Cary Eclipse, United Kingdom). Fluorescence spectra were obtained after  
192 excitation at 280 nm, scanning an emission wavelength range between 290 nm to 510  
193 nm, using 5nm excitation and emission slits wavelength. The data was collected by  
194 Cary Eclipse software version 2 (Varian Cary Eclipse, United Kingdom). Samples of  
195 native  $\beta$ -Lg, heated  $\beta$ -Lg nanoparticles, and caffeine loaded  $\beta$ -Lg nanoparticles were  
196 analysed in duplicate at a constant temperature of 20°C.

197

#### 198 **2.2.7. Stability against dissociating buffers**

199 All samples and buffers were filtered by 0.45  $\mu$ m filter before the incubation with  
200 dissociation buffers.  $\beta$ -Lg nanoparticle dispersions were mixed with equal volume of  
201 various dissociating buffers: (i) 10M urea; (ii) 0.1M Mercaptoethanol; (iii) 1% (w/v)  
202 SDS; (v) 0.1 M DTT. Dispersions were incubated for 60 min with each buffer and  
203 then particle size was measured following the method described in section 2.2.3.

204

205

#### 206 **2.2.8. Zeta potential**

207 Zeta potential of nanoparticle samples was measured by Dynamic light scattering  
208 technique using Zetasizer Nano Z in Electrophoretic Light Scattering mode (Malvern  
209 Instruments Inc., Malvern, United Kingdom) at  $25 \pm 0.1^\circ\text{C}$  and five measurements were  
210 taken for each sample. A folded capillary cell (DTS1070) was used to measure the zeta  
211 potential. The cell was washed by ethanol and deionised water before each  
212 measurement.

213

#### 214 **2.2.9. Caffeine determination by HPLC**

215 An isocratic Reversed phase High Performance Liquid Chromatography (RP-HPLC)  
216 equipped with Gilson Model 302 Pump, CE212 Variable wavelength ultraviolet  
217 detector and Hewlett Packard 3396A integrator was used to quantify the caffeine  
218 concentration contained in permeate. The column used was Ace 5 C18, 25cm  $\times$  4.6mm

219 (Hinchhrom Limited, United Kingdom, particle size 5 $\mu$ m), operated at 25  $\pm$  1 $^{\circ}$ C, the  
220 flow rate was 1.0 mL/min, with 50 $\mu$ L injection volume, while mobile phase comprised  
221 of methanol/water (50/50). Absorption wavelength was selected at 273 nm, which is  
222 the maximum wavelength for caffeine. Standard solutions of caffeine were prepared in  
223 deionized water in a range of concentrations from 0.001% to 0.01% (w/v). A standard  
224 calibration plot was prepared by plotting concentration versus area from which the  
225 concentration of caffeine was determined in a range of samples.

226

#### 227 **2.2.10. Encapsulation efficiency**

228 To study the encapsulation efficiency of caffeine into  $\beta$ -Lg nanoparticles, the caffeine  
229 encapsulated by the  $\beta$ -Lg particles was separated from free caffeine by centrifugal  
230 ultrafiltration membranes of 50KDa MWCO, Vivaspin $^{\circledR}$  20 (Sartorius Stedim Biotech,  
231 Germany). To quantify the amount of free and entrapped caffeine, 5 ml of protein and  
232 caffeine solution prepared according to section 2.2.2 was sampled and centrifuged for  
233 30 min at 2000 rpm. The retentate was removed carefully by pipette for further analysis  
234 while the permeate was used for determination of free caffeine using RP-HPLC. The  
235 amount of the entrapped caffeine was determined based on the determination of free  
236 caffeine in the permeate and by applying a mass balance. The entrapment efficiency of  
237 caffeine was calculated based on the following equation:

238

239

$$240 \text{ Entrapment efficiency (\%)} = \frac{\text{mass of caffeine entrapped}}{\text{original mass of caffeine}} \times 100 \quad (\text{Eq.1})$$

241

242

243

#### 244 **2.2.11. In-vitro gastrointestinal digestion**

245 **Gastric digestion.** The *in-vitro* gastric model protocol was adapted from Zeece *et al.*  
246 (2008) and Sarkar *et al.* (2009) with some modifications introduced here. Simulated  
247 gastric fluid (SGF) containing 2g of NaCl and 7 mL of HCl, without the addition of

248 pepsin was diluted to 1 L and pH adjusted to 1.2 using 1.0M HCl. Afterwards, 14.93  
249 mg of pepsin enzyme was added to 7 ml of SGF and held at 37°C with continuous  
250 shaking at 95 rpm in a temperature-controlled water bath (Grant OLS 200, Grant  
251 Instrument, United Kingdom) to mimic the conditions in the stomach. The pH and  
252 temperature were continuously monitored and controlled.

253

254 Caffeine-loaded  $\beta$ -Lg nanoparticles and pure  $\beta$ -Lg nanoparticles separated from 14 mL  
255 suspensions by ultrafiltration (UF) (as described in section 2.2.11) were re-dispersed in  
256 14 mL of SGF. Then 7 mL of SGF containing pepsin was added to the mixture to make  
257 up a final volume of 21 mL (protein: enzyme ratio 1.87:1 w/w). The mixture was  
258 incubated at 37°C for up to 2h and samples were withdrawn at different time intervals  
259 for particle size measurement and RP-HPLC analysis. The pH of the mixture was  
260 maintained at 1.5 using 1M HCl. The digestion reaction was terminated by raising the  
261 pH to 8 with 0.1M NaOH prior to any analysis.

262

263 **Gastrointestinal digestion.** This method was based on a digestion protocol according  
264 to Mills et al (2008) and Maccaferri et al (2012) with some modifications. A 15ml  
265 dispersion sample containing nanoparticles with and without caffeine was adjusted to  
266 pH 2 by using HCl (6M) and mixed with 2.5ml 0.1 M HCl which contained 0.27g  
267 pepsin (protein: pepsin ratio 1:9 w/w). The solution was incubated in the 37 °C water  
268 bath with a shaker at 95 rpm for two hours. A 0.1 ml sample was taken for analysis of  
269 released caffeine by HPLC. Then the rest of the sample was mixed with 12.5ml  
270  $\text{NaHCO}_3$  in which 56mg pancreatin (protein: pancreatin ratio 1.07:2 w/w) (P3292,  
271 Sigma; 4UPS) and 0.35g bile (protein: bile ratio 1:11.7 w/w) (B 8631, Sigma) were  
272 dissolved and the pH of the sample was adjusted to 7 using NaOH (6M). Samples were  
273 incubated for three hours. After small intestinal phase incubation samples were filtered  
274 through a 0.45 $\mu\text{m}$  filtration unit and analysed by HPLC to determine the caffeine  
275 released.

276

277

278 **2.2.12. Caffeine adsorption isotherm**

279 To describe the caffeine adsorption process to  $\beta$ -Lg nanoparticles and native protein the  
280 experimental data were fitted to Langmuir adsorption model:

281 (1)  $Cad = Cad_{max} \cdot k \cdot C / (1 + k \cdot C)$

282

283 where,  $Cad$  is the caffeine adsorbed to  $\beta$ -Lg per protein at equilibrium ( $\text{mg mg}^{-1}$   
284 protein),  $Cad_{max} \cdot k$  is the maximum amount of caffeine absorbed to  $\beta$ -Lg ( $\text{mg mg}^{-1}$   
285 protein) ,  $C$  the concentration of caffeine free in solution at equilibrium ( $\text{mg ml}^{-1}$ ) and  
286  $k$  the adsorption constant ( $\text{ml mg}^{-1}$ ).

287

288 **2.2.13. Calculations and Statistical Analysis**

289 Calculation of the net charge of  $\beta$ -Lg at different values of pH was performed with the  
290 online “protein calculator v3.4” software (<http://protcalc.sourceforge.net>) using the  
291 sequence of  $\beta$ -Lg. The results were statistically analysed by analysis of variance using  
292 IBM<sup>®</sup> SPSS<sup>®</sup> Statistics version 20.0. Means and standard deviations from at least three  
293 measurements carried out on two freshly prepared  $\beta$ -Lg nanoparticles were repeated.  
294 The significance level was set at 0.05. Data fitting of experimental data to models was  
295 performed with Solver from Excel MS Office 2013 (Microsoft Corporation, Redmond,  
296 WA, USA).

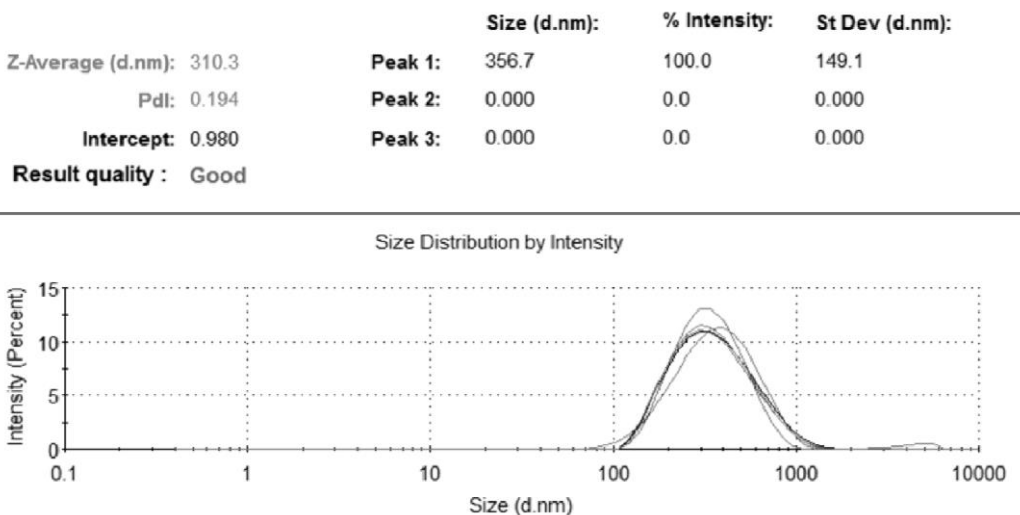
297

298 **3. Results and Discussion**

299 **3.1. Effect of pH, temperature and heat time on  $\beta$ -Lg nanoparticles**

300 Native and heated  $\beta$ -Lactoglobulin ( $\beta$ -Lg) solutions were prepared 0.2% (w/v) and pH  
301 adjusted near to their isoelectric point (pH 6.0). All samples appeared to be transparent  
302 initially. Also there was only slight turbidity after pH adjustment in agreement with  
303 observations previously reported (Chanasattru, Jones, Decker, & McClements, 2009;  
304 Mehalebi, Nicolai, & Durand, 2008; Nicolai et al., 2011; Zimet & Livney, 2009). High

305 turbidity after heating at 75°C for 45 minutes appeared to provide a rough quantitative  
 306 indication of protein aggregation in the system. A monodisperse particle size  
 307 distribution was obtained consistently with particles of an average diameter about 200  
 308 nm to 300nm. (See Fig. 1).



310 *Figure 1. The example of particle size result by DLS for nanoparticles produced at pH*  
 311 *6 and heating at 75 °C for 45 mins.*

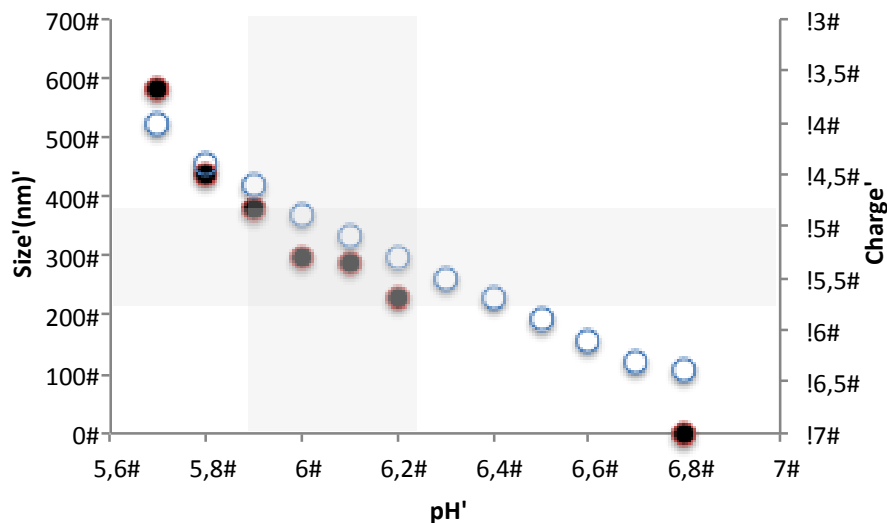
### 312 **3.1.1. Effect of pH**

313 Near the isoelectric point (pI) of the protein the overall charge is close to zero therefore,  
 314 repulsive electrostatic interactions between protein molecules will be minimised and  
 315 their aggregation will be promoted. In particular,  $\beta$ -Lg aggregation close to its pI and  
 316 under denaturing conditions was reported to produce particulate gels, which were  
 317 composed of spherical particles (Donald, 2007).

318 Here we studied the effect of a range of pH's near and above the pI on the particle size.  
 319 The pH of the aqueous  $\beta$ -Lg solution (0.2 % w/v) before pH adjustment was  $6.8 \pm 0.3$ .  
 320 At this pH, a clear solution was obtained even after heating. This pH was further away  
 321 from the pI therefore, strong electrostatic repulsive interactions between protein  
 322 molecules hindered their self-aggregation which resulted in reduced turbidity. To test  
 323 the effect of pH on protein aggregation and formation of nanoparticles samples were  
 324 incubated at pH close to the pI in the range of 5.7 to 6.2 (see figure 2). At pH 5.7 the

325 largest particle size, about 600nm, was recorded and clearly, particle size decreased  
 326 with an increase in pH. This indicated that when the pH was close to pI, and the  
 327 repulsive electrostatic forces between molecules were minimised, large particles could  
 328 be formed. Conversely, when the pH was far from the pI, the repulsive electrostatic  
 329 forces were too strong to promote aggregation and consequently smaller particles were  
 330 produced. Moreover, according to Tauliera and Chalikian (2001), within pH 5.7-6.2  
 331 only a slight change in its tertiary structure occurred but no alteration in secondary  
 332 structure. Therefore, the hidden hydrophobic parts of  $\beta$ -Lg were exposed upon pH  
 333 adjustment.

334



335

336 *Figure 2. Effect of pH in size and net charge of protein nanoparticles. Size: black*  
 337 *circles; protein charge: white circles. Experiments were carried out in duplicate and*  
 338 *mean standard deviations were 0.6-9.1 nm*

339

340 Figure 2 shows the relationship between pH and particle size and protein's net charge.  
 341 It was concluded that to form nanoparticles with size in the range of 200 nm-350 nm  
 342 and colloidal stability the pH should be strictly controlled at 5.9 to 6.2 and protein's net  
 343 charge between -5.8 to -4.8. Small changes in pH outside this range leads to small

344 changes in the protein charge but dramatic changes in particle size. So these results  
345 highlight the effect of a narrow range of pH close to the protein's pI on particle size.

346

### 347 **3.1.2. Effect of temperature**

348 The heating temperature was also found to have a significant effect on particle size at  
349 constant protein concentration. The turbidity of  $\beta$ -Lg solution heated at 50-60°C  
350 remained relatively low but increased steeply from 60-75°C. Reproducible size  
351 measurements were difficult to obtain at 65°C and a bimodal distribution was obtained.  
352 For instance, the peak of the first distribution produced with 0.2% (w/v)  $\beta$ -Lg was  
353 recorded at 3.81 nm, and the sub-population was found at 145 nm. The first population  
354 was conjectured to be native  $\beta$ -Lg which is known to have a hydrodynamic radius of  
355 around 2.5 nm (Mehalebi et al., 2008). The possible reason of obtaining such population  
356 as explained by Bauer *et al.* (Bauer, Carrotta, Rischel, & Ogendal, 2000) is that early  
357 aggregation of  $\beta$ -Lg is initiated only at 67.5°C. Significantly larger nanoparticles were  
358 formed at 75°C than at 65°C. This suggests that 65°C was not sufficient to induce  
359 complete  $\beta$ -Lg chain unfolding to produce nanoparticles in a consistent manner. On the  
360 other hand, at 75°C, a monodisperse particle size distribution was obtained consistently  
361 with particles of an average diameter about 200 nm.

362 The findings were in agreement with those by Mehalebi et al. (2008) and Gulseren et  
363 al. (2012), who found that elevated temperature could accelerate the rate of aggregation  
364 to produce larger nanoparticles. Overall the particle sizes reported here are in agreement  
365 with those reported by Donato, Schmitt, Bovetto, and Rouvet (2009), who had observed  
366 elongated compact aggregates smaller than 200 nm upon heating of 1% (w/v)  $\beta$ -Lg (pH  
367 5.9) at 75°C. Also Jones et al. (2010) had produced  $\beta$ -Lg particles ( $d < 300$  nm) with  
368 good stability to sedimentation as in this study under similar conditions. H.J. Giroux  
369 and Britten (2011) reported whey protein nanoparticles in the range of 194 nm produced  
370 at pH 5.0 using pH-cycling treatment. According to Jones et al. (2010) optimal  
371 conditions for production of  $\beta$ -Lg nanoparticles occurred when the system was heated



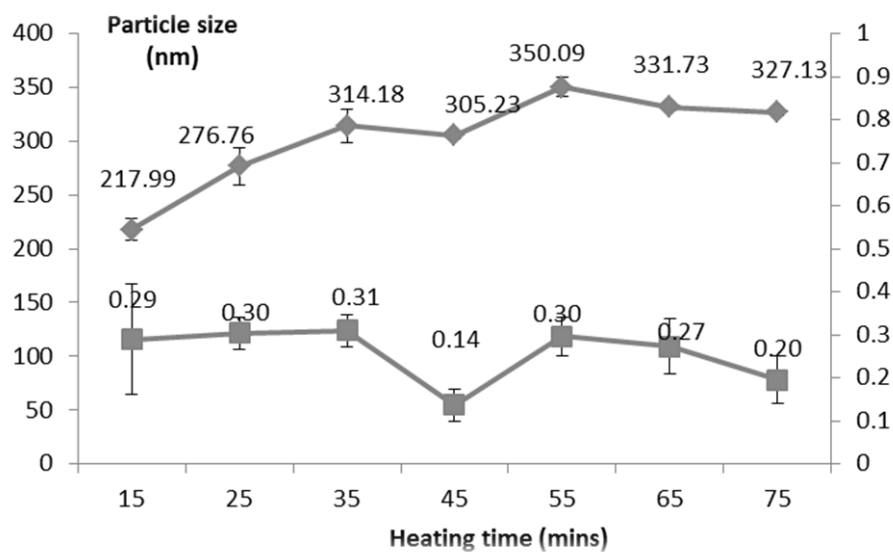
372 above thermal denaturation temperature of  $\beta$ -Lg and at a pH close to its pI which is in  
373 agreement with the above findings; these nanoparticles were reported to be irreversible  
374 protein aggregates and generally stable towards storage and pH changes.

### 375 3.1.3. Heating time

376 Besides temperature, the heating time is another factor which has a significant effect on  
377 the particle size. Previous studies suggested that long heating time promotes the  
378 formation of large aggregates. This was confirmed in the experiments carried out at  
379 varying heating times (15 to 75 minutes) but constant temperature, 75 °C (Figure 3);  
380 Note that although the water bath was at 75 °C it took about 12-14 mins for the  
381 temperature in the dispersion to reach 75 °C.

382

383 Particle size increased from 218 nm to 327 nm in the studied heating time range. The  
384 conformation structure changes might happen including the hidden hydrophobic groups  
385 at the central cavity and disulphate bonds exposing to the environment and the particles  
386 were produced. The polydispersity index (PDI) decreased and had a minimum at  
387 45mins. As shown by the low PDI number at this heating time a monodispersion was  
388 obtained.



389

390 Fig.3:  $\beta$ -Lg nanoparticle size for continuing heating (15minutes-75mintues).  $\blacklozenge$ The  $\beta$ -  
391 Lg nanoparticles size;  $\blacksquare$  PDI of nanoparticles.

392 In summary, both heating load (combination of temperature and time) and pH were  
393 found to be the key operating parameters at constant protein concentration in the  
394 production of nanoparticles of a given size. The  $\beta$ -Lg nanoparticles in the range of 200-  
395 300 nm were obtained in a consistent and reproducible manner by inducing heat  
396 denaturation and aggregation of the protein in an aqueous solution at 0.2%, pH 6.0 and  
397 75 °C for 45 minutes. At these conditions, a monodisperse size distribution was  
398 obtained and with good reproducibility.

399

400 Protein aggregation may occur due to covalent and non-covalent interactions between  
401 unfolded protein molecules. As protein denatures it will unfold to expose the  
402 hydrophobic groups as well as the reactive thiol group at Cys<sup>121</sup> which leads to protein  
403 molecules interacting via non-covalent interactions (hydrophobic interaction, hydrogen  
404 bonding) and covalent interactions (disulphide bonds) to form particles of a given  
405 microstructure.(Donato et al., 2009; Havea, Singh, & L.K., 2001). In order to obtain an  
406 insight into the physical characteristics of the nanoparticles and their microstructure,  
407 the following characterisation study was carried out.

408

## 409 **3.2 Characterisation of $\beta$ -Lg nanoparticles**

410

### 411 **3.2.1 Stability to dissociating buffers**

412 In order to get an insight into the type of the microstructure formed and the main  
413 interactions governing its formation the stability of the particles to several buffers was  
414 investigated. All samples were filtered by 0.45  $\mu$ m filter before the incubation with  
415 dissociation buffers. The effect of dissociating buffers was determined based on  
416 changes in particle size (Table 1).

417

418

419

420 **Table 1:** Effect of dissociating buffers on nanoparticle diameter (nm). The incubation  
421 time with dissociating buffers was 60 minutes.

	<i>Before</i>	<i>10M</i>	<i>1%(W/V)</i>	<i>0.1 M</i>	<i>0.1 M DTT</i>
	<i>incubation</i>	<i>Urea</i>	<i>SDS</i>	<i>2-Mercaptoethanol</i>	
<i>Particle size</i>	<i>173.0±12.5<sup>a</sup></i>	<i>234.2±1.9<sup>b</sup></i>	<i>17.41±8.8<sup>c</sup></i>	<i>176.5±0.9<sup>a</sup></i>	<i>186.1±1.5<sup>a</sup></i>

422 Experiments were carried out in duplicate, mean values with different superscript letters  
423 are significantly different at  $p < 0.05$ , the particle size before incubation is lower than  
424 200nm due to the filtration of 0.45  $\mu\text{m}$  filter.

425

426 Sodium dodecyl sulphate (SDS) interacts with proteins via electrostatic interactions and  
427 hydrophobic interactions while keeping covalent bonds intact.(Reynolds & Tanford,  
428 1970; Roy, Kumar, & Gurusubramanian, 2012). A significant reduction in particle size  
429 was observed which demonstrates that hydrophobic interactions are essential to the  
430 stabilisation of the microstructure of these particles.

431

432 Urea is a very powerful protein denaturant with the ability to break hydrogen bonds. It  
433 is considered that urea acts by breaking down protein hydrogen bonds as it interacts  
434 with peptide groups in unfolded proteins by hydrogen bonding. Interestingly, most  $\beta$ -  
435 Lg nanoparticles were not disrupted by urea. On the contrary, the particle size increased  
436 significantly as demonstrated. The swelling of the nanoparticles could be due to the  
437 formation of hydrogen bonds with the water molecules within the particles (Huppertz  
438 & de Kruijff, 2008). These results demonstrated the presence of hydrogen bonds within  
439 the internal structure of  $\beta$ -Lg nanoparticles.

440

441 2-Mercaptoethanol was added to  $\beta$ -Lg nanoparticle dispersions to cleave disulphide  
442 bonds. Interestingly 2-Mercaptoethanol had no significant effect on the size of the  
443 nanoparticles, therefore, disulphide bonds were not responsible for the microstructure  
444 formation. In order to confirm the above results, another dissociating buffer 0.1 M  
445 Dithiothreitol (DTT) was used. DTT is a dissociating buffer, which disrupts disulphide

446 bonds. The nanoparticles were stable during incubation with DTT for 60mins and even  
447 after one day (data not shown here). These results confirmed that disulphide bonds were  
448 not mainly responsible for the microstructure formation.. Various authors (Alting,  
449 Hamer, de Kruif, Paques, & Visschers, 2003; H. J. Giroux et al., 2010; Ko &  
450 Gunasekaran, 2006; Mudgal, Daubert, & Foegeding, 2011; Nicolai et al., 2011) have  
451 demonstrated the significant role of thiol-disulphide reactions in  $\beta$ -Lg aggregation but  
452 the reaction was shown to be favoured at neutral to alkaline pHs. In addition Alting *et*  
453 *al.* (Alting et al., 2003) had further ascertained the fact that disulphide bonds did not  
454 significantly contribute to the acid-induced aggregation of diluted solutions of whey  
455 protein in the initial stage of aggregation. However, partially cross-linked disulphide  
456 bonds were found in protein gels kept for a period of time, namely ageing period (Alting  
457 et al., 2003; H. J. Giroux et al., 2010; Nicolai et al., 2011). Alting et al. (2003)  
458 demonstrated that the formation of disulphide crosslinking was strongly affected by the  
459 pH (at pH 5 only 1:3160 sulphur groups is deprotonated and able to initiate  
460 thiol/disulphide exchange reactions) and protein concentration (4.5% initial protein  
461 concentration was identified as the critical value below which no significant  
462 crosslinking may occur). Since the  $\beta$ -Lg nanoparticles produced in this study did not  
463 undergo the aforementioned ageing period and the pH and protein concentrations were  
464 not favourable to disulphide crosslinking it is reasonable to conclude that disulphide  
465 bonds did not actively participate in the formation of the microstructure of the  
466 nanoparticles produced in the current study.

467

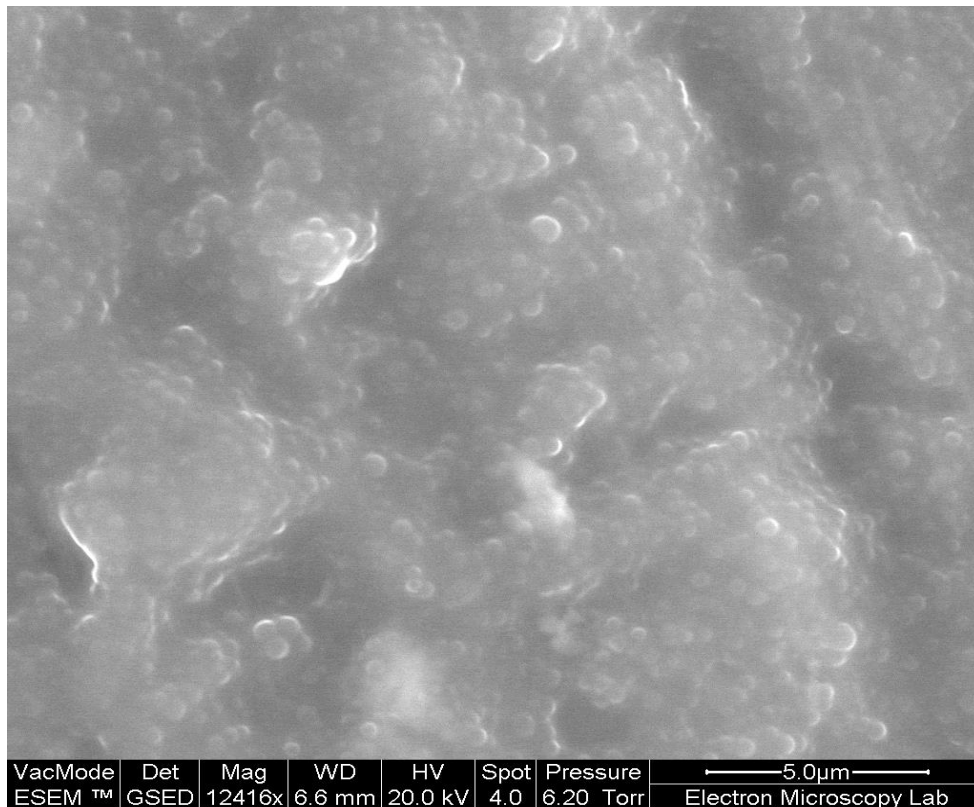
468 In summary, the predominant interactions responsible for the microstructure of the  
469 nanoparticles were found to be hydrogen bonding and hydrophobic interactions.  
470 Increased hydrogen bonding induces the formation of  $\beta$ -sheets in a protein which, is  
471 commonly found in aggregates (Gunasekaran et al., 2006). Hydrophobic interactions  
472 also played a major role in the aggregation process of  $\beta$ -Lg as expected since this  
473 protein has significant portions of hydrophobic patches, with the exact effective  
474 hydrophobicity reported to be 12.2 (Gunasekaran et al., 2006; Hansted, Wejse,

475 Bertelsen, & Otzen, 2011; Ko & Gunasekaran, 2006) and upon denaturation this area  
476 will be further exposed.

477

### 478 3.2.2. Microscope image of nanoparticle

479 To further characterise the microstructure of  $\beta$ -Lg nanoparticles environmental  
480 scanning electron microscopy was carried out on samples produced at the optimum  
481 conditions (described in 2.2.5).



483 *Figure 4: the ESEM image of  $\beta$ -Lg nanoparticles*

484 The ESEM image in Figure 4 shows spherical aggregates and in the range of sizes of  
485 those measured by DLS. This is in agreement with Krebs et al (Krebs, Devlin, &  
486 Donald, 2009) who reported the formation of spherical aggregates at the pH close to  
487 protein's pI.

488

489 Moreover, the zeta potential of these nanoparticles was determined as the key indicator  
490 of the stability of colloidal dispersions. The zeta potential of the  $\beta$ -Lg dispersion was -  
491  $37.42 \pm 2.93$  mV which indicated a moderate stable colloidal system.

492

### 493 **3.2.3 Yield of aggregation of $\beta$ -Lg**

494 In preliminary filtration experiments with an aqueous solution of  $\beta$ -Lg and a 50KDa  
495 ultrafiltration membrane, it was shown that any non-aggregated  $\beta$ -Lg permeated  
496 through the ultrafiltration membrane and thus the aggregation yield was determined  
497 based on the determination of protein concentration in the permeate by using  
498 bicinchoninic acid (BCA) method as described in 2.2.4. Nearly 93% of  $\beta$ -Lg aggregated  
499 when heated at  $75^\circ\text{C}$  for 45 min. These aggregation yields were similar to those reported  
500 by others at higher heating loads (Donato et al., 2009; H. J. Giroux et al., 2010; Moitzi  
501 et al., 2011; Mudgal et al., 2011; Schokker, Singh, Pinder, & Creamer, 2000); Giroux  
502 *et al.* (H. J. Giroux et al., 2010) reported an aggregation yield of 97.3% after heating  
503 1% (w/v) whey protein dispersion at  $80^\circ\text{C}$  for 15 min.

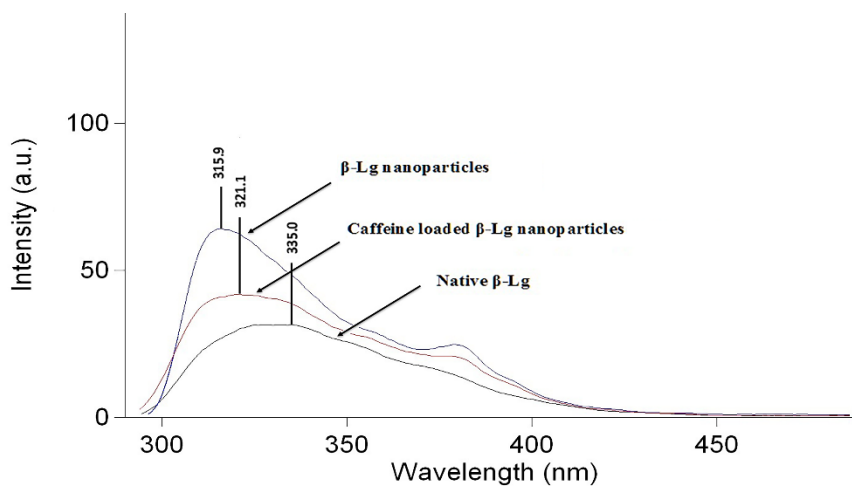
504

### 505 **3.2.4 $\beta$ -lactoglobulin conformational changes by fluorescence spectroscopy**

506 The  $\beta$ -Lg contains two tryptophan residues, Trp<sup>19</sup> and Trp<sup>61</sup>: Trp<sup>19</sup> within the cavity of  
507  $\beta$ -Lg whereas Trp<sup>61</sup> is located at the surface of the protein molecule and is close to the  
508 Cys<sup>66</sup>-Cys<sup>160</sup> disulfide bridge (Qin, Bewley, et al., 1998; Qin, Creamer, Baker, &  
509 Jameson, 1998). The X-ray crystallographic image also illustrated that Trp<sup>19</sup> is located  
510 in the interior of the  $\beta$ -Lg molecule, which is the major binding point of  $\beta$ -Lg (Sawyer  
511 et al., 1985). A mutant  $\beta$ -Lg molecule study helped to prove that Trp<sup>19</sup> was a major  
512 fluorophore of  $\beta$ -Lg in the non-polar environment (Creamer, 1995). By the influence  
513 of heat, the conformation changed at about  $50^\circ\text{C}$ , one of the tryptophans was  
514 transferred to a more polar environment accessible to solvent and above  $70^\circ\text{C}$  the  
515 second tryptophan residue became exposed to solvent. But even at  $90^\circ\text{C}$ , the second  
516 one was partially buried (Mills, 1976). Therefore in order to investigate conformational  
517 changes in  $\beta$ -Lg after heat denaturation and after caffeine encapsulation the

518 fluorescence emission spectra of tryptophan was measured (Fig. 5). An increase in the  
519 fluorescence intensity was observed for  $\beta$ -Lg nanoparticles and a fluorescence  
520 quenching effect by the caffeine upon binding to the nanoparticles. The increase in  
521 fluorescence intensity can be explained based on the exposure of previously buried Trp  
522 groups upon heating induced conformational changes in the protein.

523



524

525 *Figure 5: the fluorescence emission changes of native  $\beta$ -Lg,  $\beta$ -Lg nanoparticles and*  
526 *caffeine loaded  $\beta$ -Lg nanoparticles.*

527

### 528 3.2.5. Mechanism of nanoparticle formation

529 Based on previous studies on  $\beta$ -Lg and our observations above the following  
530 mechanism of nanoparticle formation is proposed. At neutral pH,  $\beta$ -Lg exists as dimer  
531 in aqueous solution. Upon pH adjustment (to pH 6) and heating the dimer dissociates  
532 and denatures to reactive monomers. Protein molecules start to unfold and hydrophobic  
533 groups are exposed (as shown by fluorescence measurements) which promote  
534 intermolecular non-covalent interactions (hydrophobic interactions, and hydrogen  
535 bonding) to form particles of a given microstructure as demonstrated by the stability to  
536 buffers. Although at these denaturing conditions the reactive thiol group in the protein

537 would get exposed the pH and protein concentration conditions (and lack of aging time)  
 538 used in this study did not lead to the formation of disulphide bonds and subsequent  
 539 cross-linked gel-like structure. Moreover, the spherical aggregates (as visualised by  
 540 ESEM) had a good colloidal stability which was supported by an overall strong negative  
 541 charge ( $-37.42 \pm 2.93$  mV) measured as zeta-potential.

542

### 543 3.3. Yield of caffeine encapsulation

544 The yield of caffeine encapsulation increased when caffeine to  $\beta$ -Lg molar ratio  
 545 increased reaching a maximum 13.54% at a molar ratio of 50 (mass ratio caffeine to  $\beta$ -  
 546 Lg 1:2) (Table 2). Above this maximum, a slow reduction of the percentage of caffeine  
 547 encapsulation was observed for higher caffeine to  $\beta$ -Lg molar ratio values. In addition,  
 548 caffeine-loaded particles were significantly larger than those without caffeine (over 350  
 549 nm). Li *et al.* (Li, Du, Jin, & Du, 2012) and Shpingelman *et al.* (Shpingelman, Cohen, &  
 550 Livney, 2012) had also found a similar trend for their EGCG (epigallocatechin-3-gal-  
 551 late)-loaded  $\beta$ -Lg nanoparticles.

552

553 Table 2: Caffeine encapsulation. All the encapsulation efficiency results are the  
 554 average of three replicates.

<i>Caffeine to <math>\beta</math>-Lg</i>	<i>10:1</i>	<i>20:1</i>	<i>50:1</i>	<i>100:</i>	<i>200:1</i>
<i>ratio</i>				<i>1</i>	
<i>Encapsulation efficiency (%)</i>	$10.25 \pm 1.2^b$	$11.68 \pm 3.0^a$	$13.54 \pm 3.3^a$	$10.07 \pm 2.0^c$	$9.73 \pm 0.2^d$
<i>Particle size</i>	$374.1 \pm 5.1^a$	$366.5 \pm 4.7^b$	$381.7 \pm 1.7^c$	$359.6 \pm 3.0^d$	$356.0 \pm 2.6^d$

555 Experiments were carried out in triplicate, mean values with different superscript letters  
 556 are significantly different at  $p < 0.05$

557



558 The same results were plotted as an adsorption isotherm (Figure 6) as it was  
 559 hypothesised that caffeine bound (adsorbed) the exterior of the nanoparticles up to  
 560 reaching equilibrium concentration. Interestingly it was found that the equilibrium  
 561 concentrations of caffeine bound (measured as caffeine mass per protein mass) and  
 562 caffeine free in solution followed a Langmuir type isotherm. Parameters of adjustment  
 563 of experimental data to Langmuir model are shown in Table 3.

564

565 Table 3: Adjustment of caffeine adsorption to Langmuir model

	<i>Native <math>\beta</math>-Lg</i>	<i><math>\beta</math>-Lg nanoparticles</i>
$Cad_{max}$	0,103	0,263
$k$	1,194	0,423
$r^2$	0,96332	0,96244

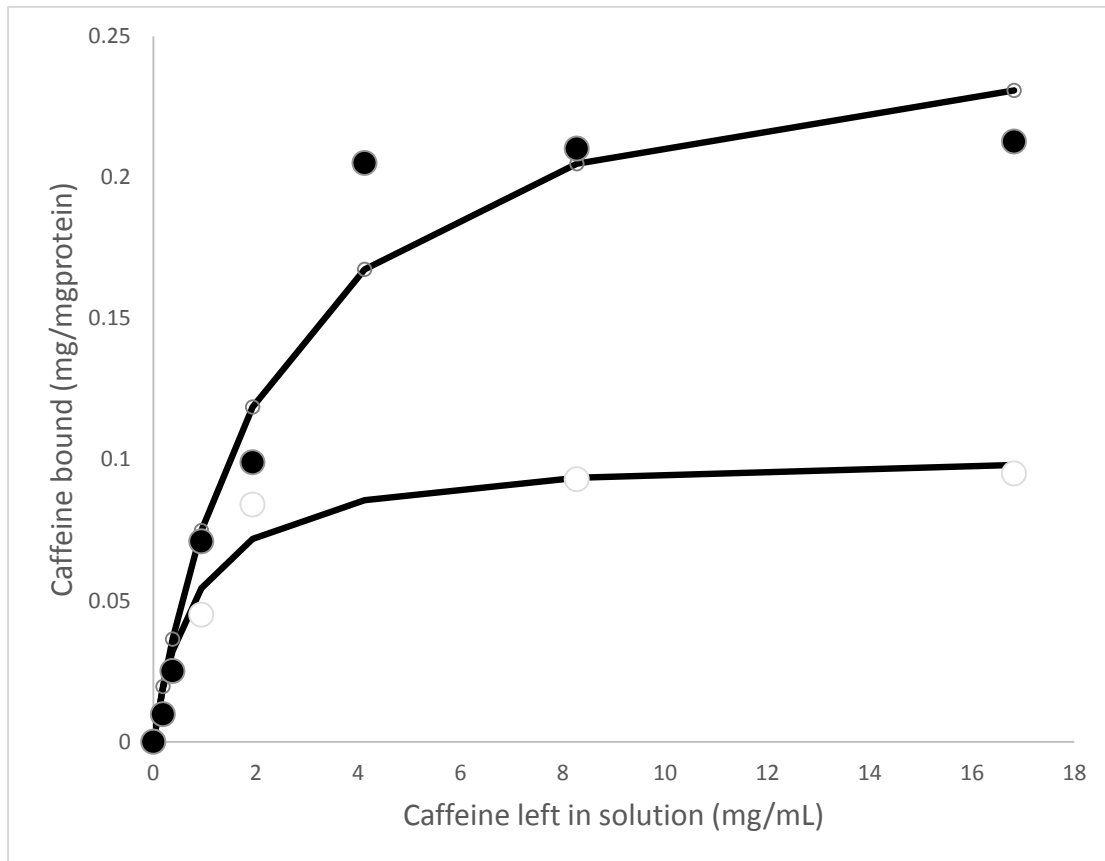
566

567 In the case of nanoparticles, a maximum binding capacity of 0.205 mg caffeine per mg  
 568  $\beta$ -Lg was found which means 19.4 molecules of caffeine per protein. However, when  
 569 the same experiments were conducted with native  $\beta$ -Lg the maximum binding capacity  
 570 was only 0.084 mg caffeine per mg protein. Additionally, caffeine had three times more  
 571 affinity for partially denatured  $\beta$ -Lg in nanoparticles than for native protein.

572 This clearly shows that the conformational change induced in the protein due to heat  
 573 denaturation led to an increase in binding capacity.

574

575



576

577 *Figure 6: Isotherm of caffeine encapsulation of native  $\beta$ -Lg (white circles) and the  $\beta$ -*  
 578 *Lg nanoparticles (black circles). Lines represent adjustment to Langmuir model.*

579

580

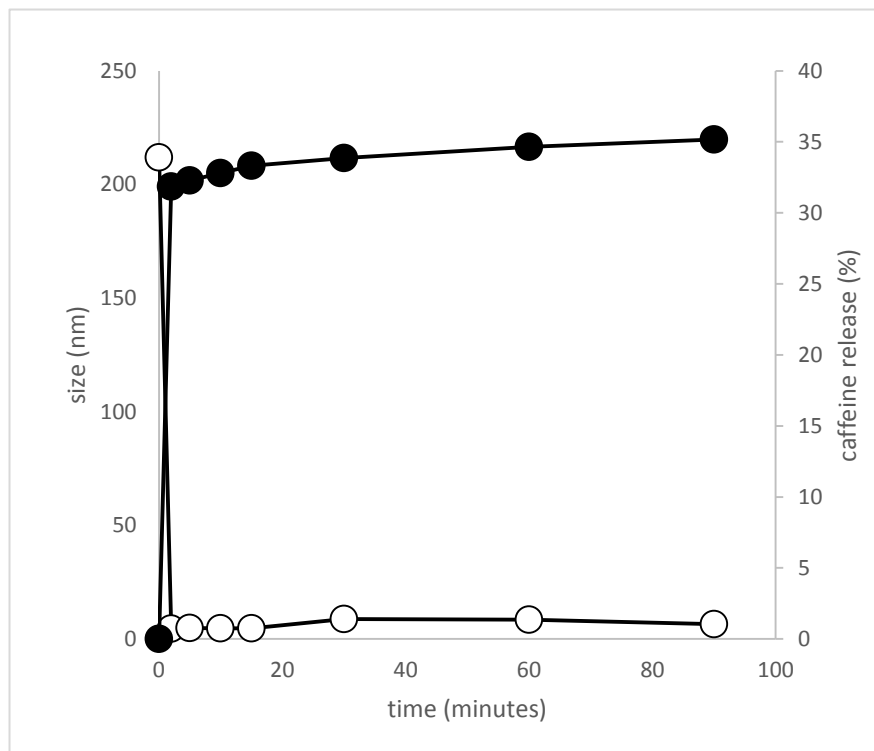
### 581 **3.5. Simulated gastric digestion**

582 The in-vitro experiment was carried out by suspending the nanoparticles containing  
 583 caffeine in simulated gastric fluid (SGF) with pepsin for 120 min under continuous  
 584 shaking at 37°C. Conditions of temperature and pH were set equivalent to the normal  
 585 gastric digestion conditions (Shpigelman et al., 2012). The protein: enzyme ratio  
 586 (1.875:1) used here was similar ratio to that reported in other works (Chen & Subirade,  
 587 2005; Sarkar, Goh, Singh, & Singh, 2009; Shpigelman et al., 2012; Zeese, Huppertz, &  
 588 Kelly, 2008). It is important to note that optimal ratio that suits the exact physiological  
 589 secretion in humans was extremely hard to establish due to the variation in gastric  
 590 secretions in different individual's health conditions and food choice (Sarkar et al.,  
 591 2009). Various protein: enzyme ratio had been proposed by Kitabatake & Kinekawa  
 592 (Kibatake & Kinekawa, 1998), Zeece *et al.* (Zeese et al., 2008); Sarkar *et al.* (Sarkar et

593 al., 2009), and Shpingelman *et al.* (Shpingelman et al., 2012) but all the authors claimed  
594 that complete hydrolysis of  $\beta$ -Lg was not achievable at any given pepsin concentration.  
595 Therefore, this ratio was chosen here to expose  $\beta$ -Lg nanoparticles to more extreme  
596 gastric conditions.

597

598 Upon addition to SGF, the pH of the  $\beta$ -Lg dispersions dropped immediately to around  
599  $\sim 1.5$  to mimic the empty stomach pH and to provide the optimum conditions for  
600 hydrolysis by pepsin. Rapid decay of particle size was observed (Figure 7) and during  
601 the incubation period polydispersity increased which can be a consequence of the  
602 unspecific action of pepsin on the peptide bonds.



603

604 *Figure 7. Black circles: Caffeine release percentage under SGF condition (all results are*  
605 *done in duplication.). White circles: Stability of  $\beta$ -Lg nanoparticles at simulating*  
606 *stomach conditions. Each of these experiments did in duplicate with standard*  
607 *deviations 2.21-3.19% for release and for size 0.80-2.33 nm*

608

609 So particle degradation happened in the first 2 minutes. At this time particle size  
610 reduced to 5 nm which corresponds to the average size of a protein dimer (Nicolai et

611 al., 2011; Sakurai , Oobatake , & Goto, 2001) and the size remained as less than 10nm  
612 with no significant difference for 60 minutes (Figure 7).

613

614 High Burst effect was observed in the kinetic of caffeine release revealing a common  
615 problem in the development of controlled release formulations when low molecular  
616 weight compounds are loaded in nanoparticles. This Burst effect seems related with the  
617 rapid nanoparticle degradation. In spite of this, high amounts of caffeine were retained  
618 in the nanoparticle (68.14% at 2 minutes) and slow and little release of entrapped  
619 caffeine was noted, even at the end of incubation (36.4%). Moreover, the gastric  
620 digestion applied in the gastrointestinal digestion experiments where lower protein to  
621 pepsin ratio was used (1: 9) than in the gastric digestion experiments (1.87:1) (see  
622 Methods), led to similar results, 36.71% caffeine released. Furthermore, almost all the  
623 caffeine was released after the small intestinal digestion phase (99.22%). Our results  
624 agreed with those of Shpigelman et al. (2012) as their  $\beta$ -Lg-EGCG complex managed  
625 to preserve 79% of their contents after 180 min of incubation in 1:20 pepsin: protein  
626 ratio solution

627 The fact that most of the caffeine is still bound to the protein after the microstructure  
628 has been destroyed indicates that the binding of the caffeine to protein is not so  
629 dependent on the microstructure but on the protein conformation and the establishment  
630 of interactions (most probably hydrophobic and hydrogen bonds) between the protein  
631 molecule and the caffeine.

632

### 633 **Conclusions**

634 One of the main outcomes of this study is that we have developed a simple method that  
635 relies in the heat denaturation of  $\beta$ -Lg and leads to the consistent production of  
636 nanoparticles of given size (average diameter 200-300) and characteristics with  
637 colloidal stability and high yield of aggregation (>93%) at the optimum conditions of  
638 pH (6) and heat load (heating at 75 C for 45 mins) which, were found to be the key  
639 operating parameters. The characterisation of the nanoparticles by a range of techniques

640 including fluorescence, DLS, and microscopy in combination with the measurement of  
641 their stability to buffers led to an improved insight of their formation and their  
642 microstructure at the optimum conditions. In summary, heat denaturation led to the  
643 protein unfolding, exposure of hydrophobic regions and subsequent formation of  
644 protein aggregates by non-covalent intermolecular interactions.

645

646 Maximum encapsulation efficiency of caffeine was 13.54% at 50:1 caffeine to  $\beta$ -  
647 Lg molar ratio. Caffeine- $\beta$ -Lg nanoparticles (~350 nm) were found significantly larger  
648 than pure  $\beta$ -Lg nanoparticles (~250 nm). Heating of  $\beta$ -Lg unfolded the non-polar region  
649 in the protein and led to an increase in binding of caffeine as compared to native  $\beta$ -Lg.  
650 Interestingly, the binding of caffeine to protein followed a Langmuir type isotherm.  
651 Both pure  $\beta$ -Lg and caffeine loaded  $\beta$ -Lg nanoparticles exhibited rapid peptic  
652 degradation but only 36.4% caffeine was released under these conditions and complete  
653 release at intestinal conditions, hence suggesting improved enteric delivery.  
654 Furthermore, both the fitting of the experimental results to a binding isotherm and the  
655 low release of caffeine even when complete disruption of the microstructure occurred  
656 suggest that caffeine binds to the unfolded protein molecule at a maximum ratio of 19  
657 molecules of caffeine per molecule of protein. Overall the 'encapsulation' efficiency  
658 was slightly better than that obtained with liposomes nanoparticles (3.8% to 9.7%)  
659 produced by Pham *et al.* (Pham, Jaafar-Maalej, Charcosset, & Fessi, 2012) utilising  
660 phospholipid and cholesterol and less than that obtained with niosomes particles  
661 produced from cholesterol and surfactant (30.4%) by Khazaeli *et al.* (Khazaeli,  
662 Pardakhty, & Shoorabi, 2007) but with significantly larger vesicle sizes (6-22 $\mu$ m).  
663 Spontaneous binding of caffeine to  $\beta$ -Lg nanoparticles could open the opportunity for  
664 the application of this milk protein as a molecular nano-vehicle to manufacture products  
665 fortified with caffeine without intense bitterness that may interfere with the original  
666 product flavour. Other potential applications include the binding of bioactives to  
667 improve their solubility and/or bioavailability.

668

669

670 **Acknowledgements**

671 Special thanks to Thong Thong Choo who initiated part of this work as an MSc project  
672 which formed the basis of the current project.

673

674 **Conflict of interest statement**

675 The author declares that there are no conflicts of interest.

676 **References**

- 677 Afferstsholt, T., & Palmer, S. (2009). Whey proteins: continued market growth despite  
678 economic crisis. *NUTRAfoods*, 8, 56-58.
- 679 Alting, A. C., Hamer, R. J., de Kruif, C. G., Paques, M., & Visschers, R. W. (2003). Number of  
680 thiol groups rather than the size of aggregates determines the hardness of cold set  
681 whey protein gels. *Food Hydrocolloids*, 17, 469-479.
- 682 Bauer, R., Carrotta, R., Rischel, C., & Ogendal, L. (2000). Characterisation and isolation of  
683 intermediates in b-lactoglobulin heat aggregation. *Biophysical Journal*, 79, 1030-1038.
- 684 C. Baldasso , T.C. Barros, & Tessaro, I. C. (2011). Concentration and purification of whey  
685 proteins by ultrafiltration. *Desalination*, 278(1-3), 381-386.
- 686 Chanasattru, W., Jones, O. G., Decker, E. A., & McClements, D. J. (2009). Impact of cosolvents  
687 on formation and properties of biopolymer nanoparticles formed by heat treatment  
688 of  $\beta$ -lactoglobulin–Pectin complexes. *Food Hydrocolloids*, 23(8), 2450-2457.
- 689 ChemBK. (2017). DL-Dithiothreitol. Retrieved from <http://www.chembk.com/en/chem/L->  
690 [DTT](http://www.chembk.com/en/chem/L-DTT)
- 691 Chen, L., Remondetto, G. E., & Subirade, M. (2006). Food protein-based materials as  
692 nutraceutical delivery systems. *Trends in Food Science & Technology*, 17(5), 272-283.
- 693 Chen, L., & Subirade, M. (2005). Chitosan/ $\beta$ -lactoglobulin core -shell nanoparticles as  
694 nutraceutical carriers. *Biomaterials*, 26, 6041-6053.
- 695 Creamer, L. K. (1995). Effect of sodium dodecyl sulfate and palmitic acid on the equilibrium  
696 unfolding of bovine  $\beta$ -lactoglobulin. *Biochemistry*, 1995(34), 7170-7176.
- 697 Donald, A. M. (2007). Why Should Polymer Physicists Study Biopolymers? *Journal of Polymer*  
698 *Science: Part B: Polymer Physics*, 45, 3257-3262.

699 Donato, L., Schmitt, C., Bovetto, L., & Rouvet, M. (2009). Mechanism of formation of stable  
700 heat-induced  $\beta$ -lactoglobulin microgels. *International Dairy Journal*, 19, 295-306.

701 Gilbert, R. M. (1984). Caffeine consumption. *Prog Clin Biol Res*, 158, 185-213.

702 Giroux, H. J., & Britten, M. (2011). Encapsulation of hydrophobic aroma in whey protein  
703 nanoparticles. *Journal of Microencapsulation (Micro and Nano Carriers)*, 28(5), 337-  
704 343.

705 Giroux, H. J., Houde, J., & Britten, M. (2010). Preparation of nanoparticles from denatured  
706 whey protein by pH-cycling treatment. *Food Hydrocolloids*, 24, 341-346.

707 Gulseren, I., Fang, Y., & Corredig, M. (2012). Whey protein nanoparticles prepared with  
708 desolvation with ethanol: characterisation, thermal stability and interfacial behavior.  
709 *Food Hydrocolloids*, 29, 258-264.

710 Gunasekaran, S., Ko, S., & Xiao, L. (2006). Use of whey proteins for encapsulation and  
711 controlled delivery applications. *Journal of Food Engineering*, 83, 31-40.

712 Hansted, J. G., Wejse, P. L., Bertelsen, H., & Otzen, D. E. (2011). Effect of protein-surfactant  
713 interactions on aggregation of  $\beta$ -lactoglobulin. *Biochimica Et Biophysica Acta*, 1814,  
714 713-723.

715 Havea, P., Singh, H., & L.K., C. (2001). Characterization of heat-induced aggregates of  $\beta$ -  
716 lactoglobulin,  $\alpha$ -lactalbumin, and bovine serum albumin in a whey protein  
717 concentrate environment. *Dairy Research*, 68(3), 483-497.

718 Huppertz, T., & de Kruif, C. G. (2008). Structure and stability of nanogels particles prepared by  
719 internal cross-linking of casein micelles. *International Dairy Journal*, 18, 556-656.

720 Jauregi, P., & Wolderufael, F. (2010). Added-value protein products from whey extraction,  
721 fractionation, separation, purification. *NUTRAfoods*, 9(4), 13-23.

722 Jones, O. G., Lesmes, U., Dubin, P., & McClements, D. J. (2010). Effect of polysaccharide charge  
723 on formation and properties of biopolymer nanoparticles created by heat treatment  
724 of  $\beta$ -lactoglobulin-pectin complexes. *Food Hydrocolloids*, 24, 374-383.

725 Khazaeli, P., Pardakhty, A., & Shoorabi, H. (2007). Caffeine-loaded niosomes: characterisation  
726 and *in vitro* release studies. *Drug Delivery*, 14, 447-452.

727 Kibatake, N., & Kinekawa, Y. (1998). Digestibility of bovine milk whey protein and  $\beta$ -  
728 lactoglobulin *in vitro* and *in vivo*. *J. Agric. Food Chem.*, 46, 4917-4923.

729 Ko, S., & Gunasekaran, S. (2006). Preparation of sub-100-nm  $\beta$ -lactoglobulin (BLG)  
730 nanoparticles. *Journal of Microencapsulation*, *23*, 887-898.

731 Krebs, M. R. H., Devlin, G. L., & Donald, A. M. (2009). Amyloid fibril-like structure underlies the  
732 aggregate structure across the pH range for  $\beta$ -lactoglobulin. *Biophysical Journal*, *96*,  
733 5013-5019.

734 Li, B., Du, W., Jin, J., & Du, Q. (2012). Preservation of (-)-Epigallocatechin-3-gallate Antioxidant  
735 Properties Loaded in Heat Treated beta-Lactoglobulin Nanoparticles. *Journal of*  
736 *Agricultural and Food Chemistry*, *60*(13), 3477-3484.

737 Livney, Y. D. (2010). Milk proteins as vehicles for bioactives. *Current Opinion in Colloid &*  
738 *Interface Science*, *15*(1-2), 73-83. doi:10.1016/j.cocis.2009.11.002

739 Mehalebi, S., Nicolai, T., & Durand, D. (2008). Light scattering study of heat-denatured  
740 globular protein aggregates. *International Journal of Biological Macromolecules*, *43*,  
741 129-135.

742 Mills, O. E. (1976). Effect of temperature on tryptophan fluorescence of beta-lactoglobulin B.  
743 *Biochim Biophys Acta*, *434*(2), 324-332.

744 Moitzi, C., Donato, L., Schmitt, C., Bovezzo, L., Gillies, G., & Stradner, A. (2011). Structure of b-  
745 lactoglobulin microgels formed during heating as revealed by small-angle X-ray  
746 scattering and light scattering. *Food Hydrocolloids*, *25*, 1766-1774.

747 Mudgal, P., Daubert, C. R., & Foegeding, E. A. (2011). Kinetic study of b-lactoglobulin thermal  
748 aggregation at low pH. *Journal of Food Engineering*, *106*, 159-165.

749 Nicolai, T., Britten, M., & Schmitt, C. (2011).  $\beta$ -lactoglobulin and WPI aggregates: formation,  
750 structure and applications. *Food Hydrocolloids*, *25*, 1945-1962.

751 Pham, T. T., Jaafar-Maalej, C., Charcosset, C., & Fessi, H. (2012). Liposome and niosome  
752 preparation using a membrane contactor for scale-up. *Colloids and Surfaces B-*  
753 *Biointerfaces*, *94*, 15-21.

754 Qin, B. Y., Bewley, M. C., Creamer, L. K., Baker, H. M., Baker, E. N., & Jameson, G. B. (1998).  
755 Structural basis of the Tanford transition of bovine  $\beta$ -lactoglobulin. *Biochemistry*,  
756 *1998b*(37), 14014-14023.

757 Qin, B. Y., Creamer, L. K., Baker, E. N., & Jameson, G. B. (1998). 12-Bromododecanoic acid  
758 binds inside the calyx of bovine  $\beta$ -lactoglobulin. *FEBS Lett.*, *1998a*(438), 272-278.



759 Reynolds, J. A., & Tanford, C. (1970). Binding of Dodecyl Sulfate to Proteins at High Binding  
760 Ratios. Possible Implications for the State of Proteins in Biological Membranes.  
761 *National Academy of Sciences*, 66(3), 1002-1007.

762 Ron, N., Zimet, P., Bargaram, J., & Livney, Y. D. (2010). Beta-lactoglobulin-polysaccharide  
763 complexes as nanovehicles for hydrophobic nutraceuticals in non-fat foods and clear  
764 beverages. *International Dairy Journal*, 20(10), 686-693.  
765 doi::10.1016/j.idairyj.2010.04.001

766 Roy, V. K., Kumar, S., & Gurusubramanian, G. (2012). Protein-structure, properties and their  
767 separation by SDSpolyacrylamide gel electrophoresis *Sicencevision*, 12(4), 170-181.

768 Sakurai, K., Oobatake, M., & Goto, Y. (2001). Salt-dependent monomer–dimer equilibrium of  
769 bovine  $\beta$ -Lg at pH 3. *Protein Science*, 10, 2325-2335.

770 Sarkar, A., Goh, K. K. T., Singh, R. P., & Singh, H. (2009). Behaviour of an oil-in -water emulsion  
771 stabilised by  $\beta$ -lactoglobulin in an *in vivo* gastric model. *Food Hydrocolloids*, 23,  
772 1563-1569.

773 Sawyer, L. (2002). beta-Lactoglobulin: Properties, structure and function. *Journal of Dairy*  
774 *Science*, 85(Supplement 1), 50.

775 Schokker, E. P., Singh, H., Pinder, D. N., & Creamer, L. K. (2000). Heat-induced aggregation of  
776 b-lactoglobulin AB at pH= 2.5 as influenced by ionic strength and protein  
777 concentration. *International Dairy Journal*, 10, 233-240.

778 Shpigelman, A., Cohen, Y., & Livney, Y. D. (2012). Thermally-induced  $\beta$ -lactoglobulin-EGCG  
779 novehicles: loading, stability, sensory and digestive-release study. *Food*  
780 *Hydrocolloids*, 29, 57-67.

781 Sigma-Aldrich. (2017). 2-Mercaptoethanol  $\geq 99.0\%$  |Sigmaaldrich.com. Retrieved from  
782 31 January 2017,  
783 <http://www.sigmaaldrich.com/catalog/product/aldrich/m6250?lang=en&region=GB>

784 Somogyi, L. P. (2010). Caffeine Intake by the U.S. Population.

785 Tauliera, N., & Chalikian, T. V. (2001). Characterization of pH-induced transitions of  $\beta$ -  
786 lactoglobulin: ultrasonic, densimetric, and spectroscopic studies. *Journal of Molecular*  
787 *Biology*, 314(4), 873-889.

788 Tumolo, T., Angnes, L., & Baptista, M. S. (2004). Determination of the refractive index  
789 increment (dn/dc) of  
790 molecule and macromolecule solutions by surface plasmon resonance. *Analytical*  
791 *Biochemistry*, 333(2), 273-279.

792 Warren, J., & Gordon, J. (1966). On the Refractive Indices of Aqueous Solutions of Urea. . *The*  
793 *Journal of Physical Chemistry*, 70(1), 297-300.

794 Zeese, M., Huppertz, T., & Kelly, A. (2008). Effect of high-pressure treatment on in-vitro  
795 digestibility of  $\beta$ -lactoglobulin. *Innovative Food Science and Emerging Technologies*, 9,  
796 62-69.

797 Zimet, P., & Livney, Y. D. (2009). Beta-lactoglobulin and its nanocomplexes with pectin as  
798 vehicles for omega-3 polyunsaturated fatty acids. *Food Hydrocolloids*, 23(4), 1120-  
799 1126. doi:10.1016/j.foodhyd.2008.10.008

800